Conception of a post-correlation RFI mitigation approach based on RFI impact estimation to the correlators and comparison with the classical pre-correlation FDAF method

Thomas Kraus, Thomas Pany
Universität der Bundeswehr München - Institute of Space Technology and Applications

BIOGRAPHY

Thomas Kraus is a research associate at the Universität der Bundeswehr München and works for the satellite navigation unit LRT 9.2 of the Institute of Space Technology and Space Applications (ISTA). His research focus is on future receiver design offering a superior detection and mitigation capability of RF interferences. He holds a master's degree in Electrical Engineering from the Technical University of Darmstadt, Germany.

Prof. Thomas Pany is with the Universität der Bundeswehr München at Space Systems Research Center (FZ-Space) where he leads the satellite navigation unit LRT 9.2 of the Institute of Space Technology and Space Applications (ISTA). He teaches navigation focusing on GNSS, sensors fusion and aerospace applications. Within LRT 9.2 a good dozen of full-time researchers investigate GNSS system and signal design, GNSS transceivers and high-integrity multi-sensor navigation (inertial, LiDAR) and is also developing a modular UAV-based GNSS test bed. ISTA also develops the MuSNAT GNSS software receiver and recently focuses on smartphone positioning and GNSS/5G integration. He has a PhD from the Graz University of Technology (sub auspiciis) and worked in the GNSS industry for seven years. He authored around 200 publications including one monography and received five best presentation awards from the US Institute of Navigation. Thomas Pany also organizes the Munich Satellite Navigation Summit.

ABSTRACT

This paper introduces a concept to correct post-correlation results from the influence of radio frequency interference (RFI). Most of the single aperture GNSS mitigation algorithms are pre-correlation techniques with the objective to clean the GNSS noise floor from the RFI before the signal stream will be fed to the GNSS receiver. This new approach passes the RFI together with the noise floor and the GNSS signals to the tracking engine. The signal stream will be analyzed and the influence on the correlator outputs (punctual, early, late, each in-phase and quadrature phase) will be estimated. The estimation allows a correction of the deformed auto-correlation result, before it will be further progressed by the discriminators of the tracking unit. The performance of this method will be evaluated by a basic GNSS software receiver under the stress of a personal privacy device (PPD) and an amateur radio signal of the 23-centimeter band (also Galileo E6) as interference source. Additionally, the results will be compared with the performance of the classical pre-correlation frequency domain adaptive filter (FDAF).

I. INTRODUCTION

The vulnerability of GNSS receivers caused by radio frequency interference (RFI) is already well known [1]. Many examples have already been reported [2, 3, 4], for which reason there is no doubt that future GNSS receivers should be equipped with a higher robustness against RFI. This leads to higher requirements for GNSS receivers in terms of hardware and software. A GNSS antenna and a RF front-end needs to provide high linearity for the large RFI power without disturbing the GNSS noise [5, 6], and it should have a good out-of-band filter rejection. The last step of a front-end is the conversion to the digital domain, which furthermore can limit the instantaneous dynamic range. The degradation caused by the in-band RFI will be mitigated by digital signal processing (DSP).

DSP mitigations are mostly pre-correlation techniques with various complexity [7]. The drawback of pre-correlation methods in combination with a one input port front-end is the difficulty to separate the GNSS noise floor from the RFI. An additional input source could support the mitigation process, but increases the complexity and costs of the hardware. Array antennas are even more sophisticated, but therefore they can use spatial diversity to separate RFI from the GNSS signal.

The proposed concept in this paper only requires a one input port front-end. To achieve a higher separation between the GNSS noise floor and the RFI, the idea is to correct the RFI influence after the correlation process and to use the frequency domain for the RFI estimation. First work to correct the RFI at the post-correlation were done with very narrow-band continuous wave signals [8, 9] and was called repair algorithm based on a third order Prony model. Further work to separated the GNSS noise

 https://doi.org/10.33012/2020.17704

floor from the RFI in the frequency domain was done by [10] with the robust transform domain signal processing for GNSS.

The post-correlation and RFI correction (PCRC) presented at this paper keeps the classical tracking unit unchanged and estimates the influence of the RFI to the correlator, which is derived from the input signal stream within the frequency domain. The effect of the RFI to the correlator will be subtracted, before it will be further processed by the discriminators of the tracking unit. At this stage of work, a very simple calculation were applied and achieves not yet the performance of a classical pre-correlation frequency domain adaptive filter (FDAF). But, the potential for a better performance is demonstrated and ideas for future research are discussed.

The paper is organized as follows. Section II introduces the concept of the post-correlation RFI correction (PCRC). It provides some examples about the reconstruction of the auto-correlation function and explains the requirements to the receiver hardware and software. Section III continues with the theory of the PCRC approach, which is based on the spectral line theory. A novel correlator plot is introduced, which shows the inside of one correlation process over the frequency bin scale. Section IV provides detailed information about the test setup. A software receiver based on MATLAB® was used for the demonstration with real GNSS signals and RFI sources, which were recorded with a software defined radio. Finally, Section V shows the results with the effective C/N_0 as performance criteria, and future work is proposed.

II. POST-CORRELATION RFI CORRECTION CONCEPT

Different to pre-correlation mitigation techniques, the post-correlation RFI correction (PCRC) approach let's pass the interference through correlator branches and keeps the architecture of the classical GNSS tracking unit unchanged. The influence of the RF interference shall be estimated and subtracted after the integration and dump units (I&D units). Figure 1 shows the block diagram of the classical GNSS tracking unit and it is extended by the I&D RFI estimator. The block diagram of the RFI estimator is given in Figure 4 and two examples about the recovery of the auto-correlation function (ACF) are provided by Figure 2 and 3.

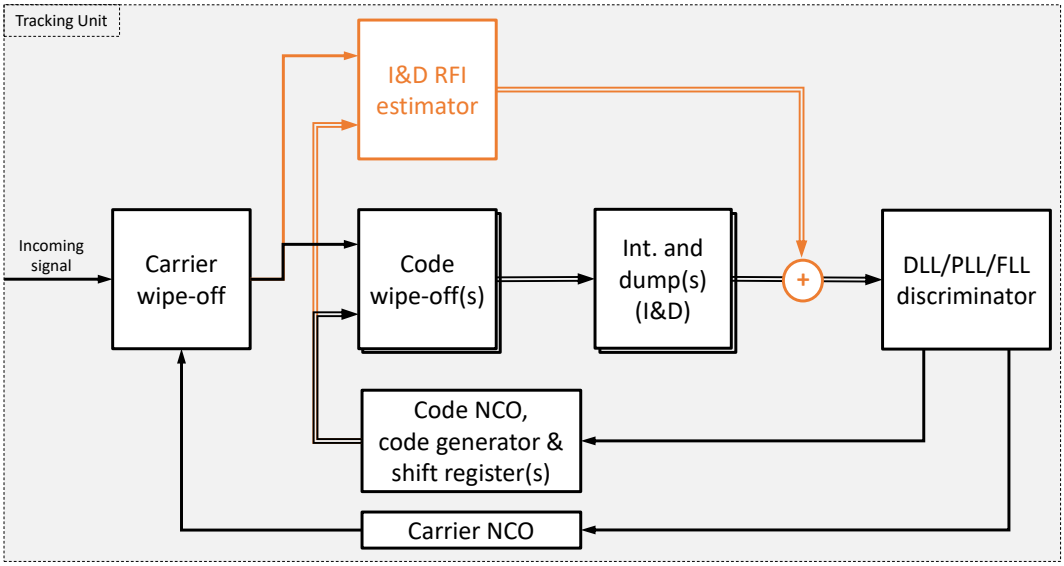

Figure 1: Block diagram of a classical GNSS tracking unit (in black color) and the post-correlation RFI correction concept (in orange)

A classical tracking unit operates the correlation within the time domain. First, the incoming signal is processed by the carrier wipe-off to get rid of the Doppler frequency. The next step is followed by the correlation process, which is compounded by the code wipe-off processes and I&D units. In a standard tracking unit, there usually exists six correlator branches for one GNSS signal and satellite: twice times the early, late, and prompt (once for the in-phase and the others for the quadrature phase). Afterwards, discriminators for code and phase are steering the code and phase numerically-controlled oscillator (NCO), respectively. Both NCOs are closing the control loop for tracking of the desired GNSS signal.

RF interference influences the correlator values, which leads to higher errors up to loss-of-lock after a certain RFI power level. The theory of how the correlator values are manipulated is described in the next section. The aim with the PCRC method is to estimate this influence, which will be inversely added to the I&D values (see orange block of Figure 1). An early-minus-late correlator needs a stable ACF, which is deformed by RFI. Figure 2 and 3 shows this influence by a frequency modulation (FM) signal and a personal privacy device (PPD) as interference, respectively. In normal operation, the full energy of the GNSS signal is in the in-phase branch of the prompt correlator after a stable phase locked state. The blue line plots the output of the in-phase prompt correlator. The red line demonstrates the estimate of the interference component. In case of this FM signal, the shape is like a sinusoidal curve, which is typical for a continuous wave narrow-band signal. This is caused by the phase changes occurring

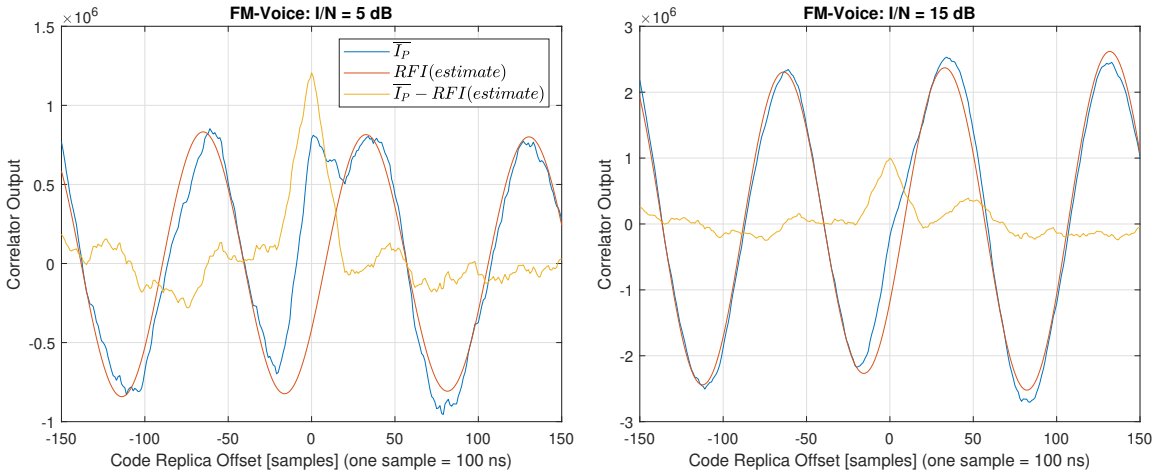

Figure 2: Output of the in-phase prompt correlator (blue), the estimation of the RFI influence (red), and the correction (yellow) with a GPS L1-C/A ($C/N_0 = 55$ dB-Hz, $T_{int} = 1$ ms) and a FM-Voice signal with an interference-to-noise ratio of (a) 5 dB and (b) 15 dB

by shifting the code replica. By the subtraction of the correlator output and the RFI estimate (yellow curve), the ACF is recovered again. In case of higher power of the interference or in conjunction with broadband interference, the ACF is not directly visible anymore, but can be reconstructed with a certain quality by the PCRC method. Even though a PPD as used for Figure 3 is a narrow-band signal with a fast frequency change over a large bandwidth [11, 12], it behaves for a correlator like a broadband signal.

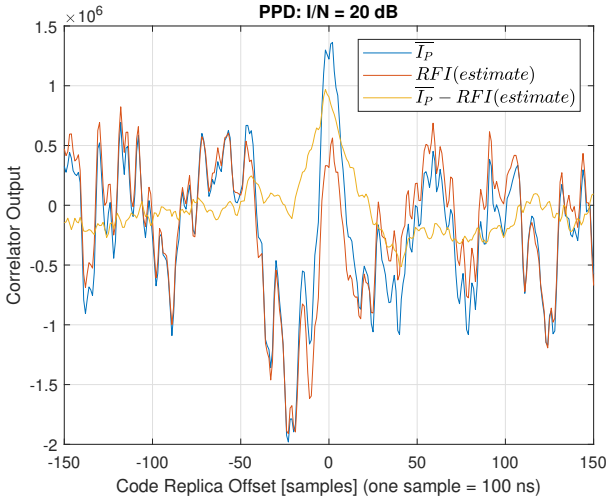

Figure 3: Output of the in-phase prompt correlator (blue), the estimation of the RFI influence (red), and the correction (yellow) with a GPS L1-C/A signal ($C/N_0 = 55$ dB-Hz, $T_{int} = 1$ ms) and a Personal Privacy Device (PPD) with an interference-to-noise ratio of 20 dB

The estimation of the RFI influence to the correlator is done by the I&D RFI estimator shown in Figure 4 and occurs in the frequency domain. Therefore, the baseband signal stream after the carrier wipe-off process will be transformed by a discrete Fourier transform (DFT) or FFT, if applicable. It should be said here, that the direct signal stream before the carrier wipe-off process could also be selected for the estimation, but it would increase the complexity for this paper unnecessarily. The next step is the selection of the highest frequency bins, which exceeds a fixed threshold level. The selected frequency bins will be used to calculate the RFI influence to the I&D units according to equation (1) and (2), which needs the frequency transformation of the corresponding code replica. It is also possible to use pre-calculated memory based values selected by the code NCO value to save computational resources by replacing an always repeating function for each correlation interval. Furthermore, the shift of the code replica could also be calculated in the frequency domain directly. The phase components are directly dependent to the shift of the code and the amplitude components remain constant. A drawback with this type of selection and calculation is, that the GNSS signal energy of the selected frequency bins are not separated from the RFI components, which leads to a certain degradation of the reconstructed ACF (or even more correct: the corresponding early, prompt, and late I&D values). The PCRC

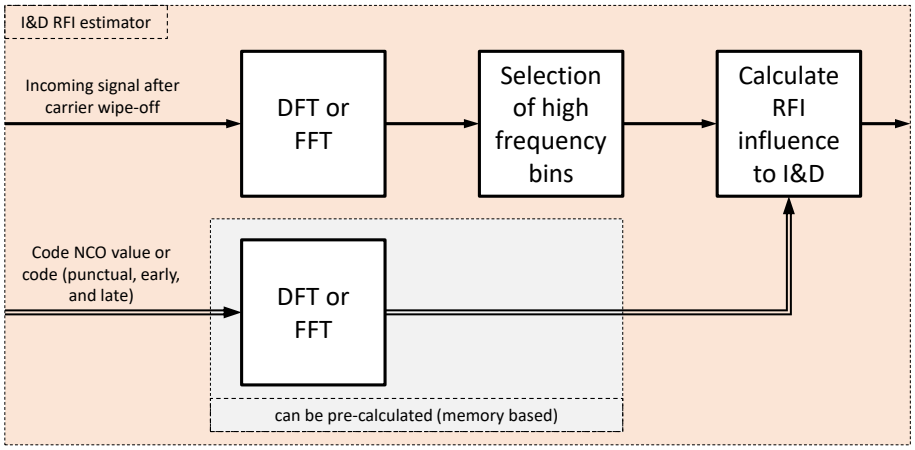

Figure 4: Block diagram of the post-correlation (I&D) RFI estimator

does not need a inverse transformation, because the influence of the inference to the time domain will be directly calculated from the frequency domain.

Requirements to the receiver hardware and software

The RF front-end of the GNSS receivers needs a high linearity in the RF signal conditioning and a high-bit resolution of the digital signal, so that the front-end can provide a very large instantaneous signal dynamic for the RFI. Otherwise, the hardware would be the limiting factor of the robustness [6]. But, this requirement is also valid for other DSP mitigation methods. The pre-correlation mitigation techniques will reduce the energy of the RFI, so that afterwards the digital amplitude resolution can be decimated to the common low-bit resolution for GNSS [13] by a digital automatic gain control. This means, that a tracking unit will normally have a maximum digital amplitude resolution of up to four bits. The introduced post-correlation and RFI correction methods feeds the entire bit resolution through the correlation process up to the I&D units. From a SDR like the USRP, we get a integer resolution of 16 bits, whereas the built-in ADC just support up to 14 bits. A hardware implementation tries to minimize the number of bits, because they drives the implementation costs. The software receiver of our institute called MuSNAT [14] already uses 16 bit as input values for the multiplication for the standard correlator and 8 bit for the fastest correlator [15]. Additionally, the estimator needs for each correlation process a DFT or FFT of the samples for each signal and satellite, when RFI interference is present.

III. THEORY OF THE POST-CORRELATION RFI CORRECTION

To understand the theory of the post-correlation RFI correction, we need to dive slightly into the spectrum line theory. The consideration of spectral lines is the exactest way of calculation for the RFI influence to the GNSS signal. Another model as introduces by [16] is easier, but it is using an average power estimation of the spread spectrum modulation. The spectrum line theory can also reflect the phase of the code replica and interference component. A very exact model is essential for a RFI correction algorithm, whereas the average model is by far good enough for an estimation of the RFI influence to the output values of GNSS receivers (in particular the effective C/N_0).

There were a lot of work done in the last decades to investigate the spectral line influence on a GNSS receiver. The first papers [17, 18, 19, 9] were using the sinc-function, whereas [20] changed it to $sinc^2$. Others followed the introduced $sinc^2$ [21, 22, 23]. All of them except of the very first ones - at least in their equations - are using just the nearest spectral line of the code. In this case, the spacing to the nearest spectral line of the code is applied. Directly after the correlation process at each I&D unit, this model is not mature enough anymore. There is simply no spectral line in between of the code replica, which is digitized with the same parameters as the incoming signal samples. Any RF interference with a spectrum in between of two spectral lines in the analog domain is decomposed to nearby spectral lines in the digital domain.

Figure 5 illustrates the spectrum and the prompt correlator output after the I&D unit, which is arbitrarily zoomed in between of 40 to 45 kHz. The RF-interference is a single-tone continuous wave signal (cosine) with a fixed phase ϕ_{int} of 0° and a constant amplitude equal to the code replica, but it has an adjustable frequency f_{int}. The in-phase branch gets the same phase of 0°, and the quadrature branch has a phase shifted by 90°. The phase of the PLL is assumed to be 0°. Any other phase value of the PLL would lead to an additional phase offset of both correlator branches. The absolute output value of the in-phase correlator $\overline{I}_P$ (blue curve) and the quadrature correlator $\overline{Q}_P$ (red curve) will show a different behavior because of their phase difference. It should be noted, that these results are the one of the punctual correlators, but without a GNSS signal and a noise source as input source. Therefore, the early and late correlator outputs would look similar. The green curve plots the auxiliary function $\sqrt{\overline{I}^2 + \overline{Q}^2}$, which is used for most of the code discriminator function. In contrary to the in-phase and quadrature results, the output of the

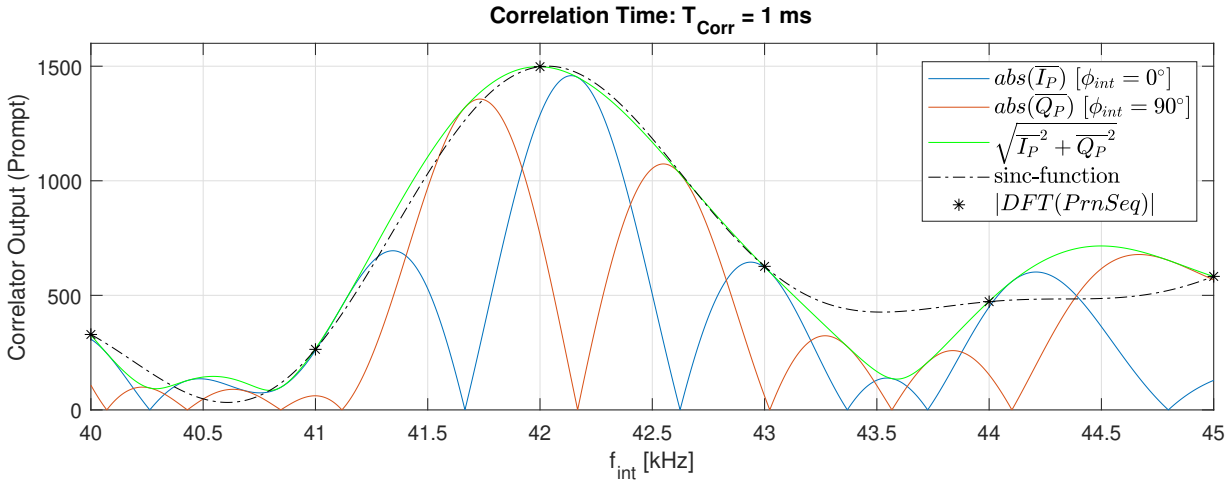

Figure 5: Correlator outputs, auxiliary function as used for the code steering and the C/N_0-estimation, the model with sinc-function, and the Fourier transform of the code replica with GPS L1-C/A PRN 1 (the input signal is a single-tone continuous wave signal with an adjustable frequency f_{int})

auxiliary function is always equal for any phase offset of the single-tone continuous wave interference. The "$sinc$-function" commonly used to model the interference effect on a GNSS receiver does not fit perfectly to the reality but is still better than the "$sinc^2$-function". The discussion about the error is out of scope for this paper. Nevertheless, the error comes from the fact, that the continuous wave signal is decomposed to the nearby spectral lines and the model based on the distance to the next spectral line is imprecise. That's why, the Fourier transform of the code replica (see asterisk dots) matches exactly the auxiliary function and the $sinc$-function. With these information, we can calculate the influence of the interference in the following way:

$$\overline{I_P}\,[n] = \sum_{k=0}^{0.5 \cdot N_{SP}} |SP_I(k)| \cdot \Re\left\{C_{T_{\text{int}}}(k) \cdot e^{-i \cdot \phi_{SP_I}(k)}\right\} \tag{1}$$

$$\overline{Q_P}\,[n] = \sum_{k=0}^{0.5 \cdot N_{SP}} |SP_Q(k)| \cdot \Re\left\{C_{T_{\text{int}}}(k) \cdot e^{-i \cdot \phi_{SP_Q}(k)}\right\} \tag{2}$$

$$SP_I\,[n] = DFT\left(\Re\left\{sp_{RFI}\,[n] \cdot e^{-i \cdot (2\pi f_{cb} + \phi_{cb})}\right\}\right) \tag{3}$$

$$SP_Q\,[n] = DFT\left(\Im\left\{sp_{RFI}\,[n] \cdot e^{-i \cdot (2\pi f_{cb} + \phi_{cb})}\right\}\right) \tag{4}$$

where:

- $sp_{RFI}\,[n]$ is the n-th sample package of the RFI before the carrier wipe-off process
- N_{SP} is the length of the sample package
- $C_{T_{\text{int}}}(k)$ is the discrete Fourier transform of the code replica or replicas (the concatenation of the same code(s) for a longer integration time)
- f_{cb} is the frequency of the carrier for the conversion to the baseband
- ϕ_{cb} is the phase of the carrier for the conversion to the baseband
- ϕ_{SP_I} and ϕ_{SP_Q} is the phase of SP_I and SP_Q, respectively

These equations assume, that we know the RFI from the sample package $sp_{RFI}\,[n]$. In reality, the incoming signal $sp_{in}\,[n]$ is mixed with the RFI, GNSS signal, and the noise floor. The algorithm in this paper just selects the frequency bins higher than a pre-defined threshold SP_{thres} and replaces $sp_{RFI}\,[n]$ with the incoming samples to the tracking unit $sp_{in}\,[n]$. All the frequency components, which are below of the threshold, will be ignored or mathematically set to zero as indicated by the following equations:

$$SP_I(k) = \begin{cases} SP_I(k), & if\ |SP_I(k)| > SP_{thres} \\ 0, & otherwise \end{cases} \tag{5}$$

$$SP_Q(k) = \begin{cases} SP_Q(k), & if\ |SP_Q(k)| > SP_{thres} \\ 0, & otherwise \end{cases} \tag{6}$$

$$\forall k \in \mathbb{N}_0 \wedge k <= \frac{N_{SP}}{2}$$

As already said, the drawback of this selective threshold method is, that the energy of the GNSS signal with the selected frequency bins gets also lost with this approach.

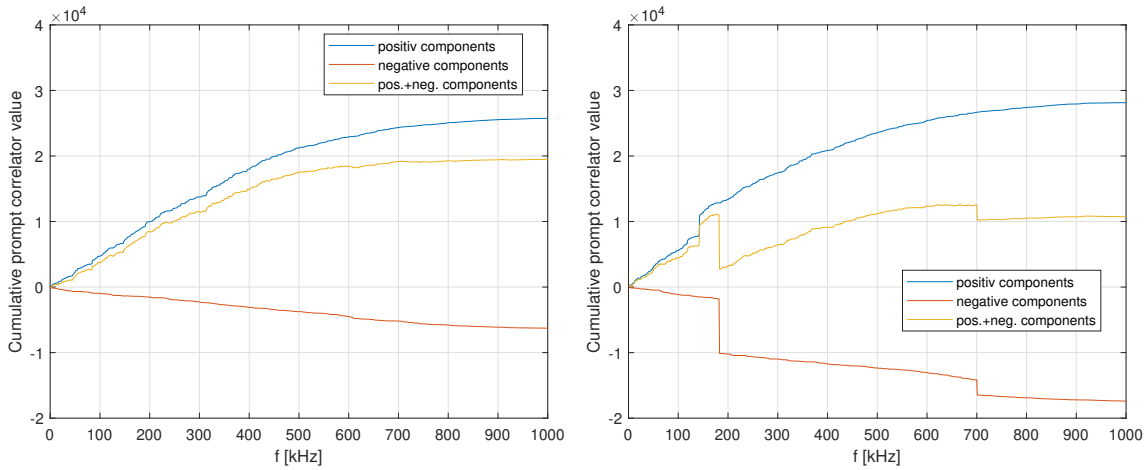

Figure 6: Cumulative prompt correlator value of the in-phase branch with spectral line components up to one MHz for a GPS L1-C/A signal: (a) no RFI, and (b) three spectral line interference at 142, 182, and 700 kHz

Figure 6 illustrates the influence of three spectral line RFIs. This plots are very unusual in today's publications and shows a kind of *"inside of a correlator"* on the frequency domain. The left plot is without RFI and the right plot is affected by three spectral line interference at 142, 182, and 700 kHz. The x-axis is here limited to one MHz for a better visualization. The rest of the frequency components will effect the lines only marginal, because with a GPS L/1-C/A most of the energy is obtained by the main lobe. The y-axis shows the cumulative values of the prompt correlator output after the I&D unit for the in-phase branch. Here, the PLL is locked to the phase, so that all the energy of the GPS L/1-C/A signal is entirely in the in-phase branch. The summation along the frequency axis is separately done once for the positive and additional for the negative frequency correlation component. In case of a pure GNSS signal without any noise, the negative components would always be zero. Here, the noise is distributed randomly but homogeneous to the positive and negative components. Both components together (yellow curve) indicates the correlation process in the frequency domain. The time domain correlator gets only the final result, which is the cumulative value of the positive and the negative components together at the highest frequency. Finally, Figure 6(b) demonstrates the influence of RFI spectral line interference. The first spectral line interference at 142 kHz causes a jump into the positive direction. Whereas, the interference at 182 and 700 kHz generate a jump into the negative direction. This leads to an error to the final correlator result, which shall be corrected by the PCRC method. It shall be repeated again, that that kind of interference is just for the demonstration and exists not in any real RFI situation. Even when a single spectral line interference would exists, the RF signal chain of the GNSS receiver would already modify this spectral line to a broader spectrum and finally the digitization would require a perfect synchronization to the RFI. Additionally, any frequency correction by the carrier wipe-off process to remove the Doppler frequency from the GNSS signal would lead to a segmentation of the single RFI spectral line to adjacent spectral line components.

IV. TEST SETUP

In this section, the test setup is described, which is used for the demonstration of the PCRC concept. As performance metrics, the effect on the C/N_0 is evaluated in dependence to the I/N as shown in Figure 8 and 9.

Front-end and Signal Recording

The software defined radio USRP-2952 from National Instruments were used as RF front-end. Real GNSS-RF-samples were recorded with a GNSS antenna without any RF interference. In this paper, we compare the GPS L1-C/A signal with a personal privacy device (PPD) and the Galileo E6-C signal with a narrow-band amateur radio signal. All the signals were recorded with a complex sampling and a sampling rate of 10 MHz to get a bandwidth of 20 MHz. The recording was done on the 09.03.2020 at 4:08 pm. The strongest GPS L1-C/A and Galileo E6-C signal was selected with the PRN 25 and SVID 1, respectively. The RFI samples were directly recorded from the PPD and amateur radio device with the same SDR. Later, they are digitally merged and tuned for the different interference-to-noise ratios.

Software Receiver

For the demonstration and comparison of this post-correlation approach, the software receiver of *Kai Borre et al.* were used [24]. This gives other researchers the possibility to reconstruct the results. This receiver is very basic, but for our purpose more than good enough, and the implementation can be easily modified thanks to MATLAB®. The receiver had been adapted for complex samples [25] and a C/N_0-estimator was implemented according to the concept of *Ward* [26] with an additional correlator branch just for the noise floor estimation. Additionally, the acquisition and tracking capability for Galileo E6-B/C were added with the codes of [27]. The mentioned post-correlation RFI correction approach was implemented and will be compared with the classical FDAF pre-correlation technique. The implementation of the FDAF was done according to [28, 29] with a FFT depth of 1024, an overlap of 50%, and a Hanning window. The FDAF was not synchronized to the tracking unit.

Type of Interference

In this paper, we compare the GPS L1-C/A signal with a personal privacy device (PPD) and the Galileo E6-C with a narrow-band amateur radio signal. Detailed studies about PPDs were done in [11, 12]. PPDs are a very complex type of RFI for a tracking unit because of it very fast sweep time, which appear for a GNSS correlator as a broadband signal. Our PPD is of class II (FM-signal with one saw-tooth function) transmitting in the E1/L1-band with a bandwidth of 12.18 MHz and a sweep time of 14.48 µsec, whereas the chirp up- and down-time is 6.83 and 7.65 µsecs, respectively. It is shown in Figure 7(a).

(a) **(b)**

Figure 7: Used RFI for the tests: (a) Personal Privacy Device, and (b) YAESU FT-736R (FM/SSB Amateur Radio Receiver) *[Source: https://www.universal-radio.com/catalog/hammulti/ft736r.html]*

The second signal source is a narrow-band amateur signal of group 2 as used in the measurement report about a potential coexistence of amateur radio service and Galileo E6 [30]. It should be noted that there is no discussion and evaluation about the on-going co-existence discussion done on CEPT level within this paper [31]. Here, this signal is just used for academic research consideration. It is a FM signal with a test sentence of pre-recorded voice repeating the spoken names of German cities („Berlin, Hamburg, München, Koblenz, Leipzig, Dortmund"). The hissing sounds within those names ensure that the voice spectrum is equally balanced over the full audio bandwidth [30]. The occupied bandwidth (99%) is 11.1 kHz. The audio sequence was repeated without interruption during the full test period. This FM-voice signal was transmitted by the all-mode transceiver of YAESU with the model number FT-736R, which is displayed in Figure 7(b).

V. RESULTS AND DISCUSSION

The performance of the GNSS receiver is depicted with the effective carrier-to-noise ratio [16, 32], which was directly estimated by the prompt and noise correlator outputs. This provides the capability to compare the quality of the countermeasures by the post-correlation RFI correction (PCRC) and the classical frequency domain adaptive filter (FDAF). The FM-voice as interference in conjunction with Galileo E6-C is given in Figure 8 and the PPD in conjunction with the GPS L1-C/A is plotted in Figure 9.

Tests were also done by rotating the configuration scenario, but they are not presented in this paper because of similar results. There would not be an additional benefit and the amateur signal is only occurring in the E6-Band whereas the PPDs are more present in the L1/E1-Band. The integration time for both signals was set to one millisecond.

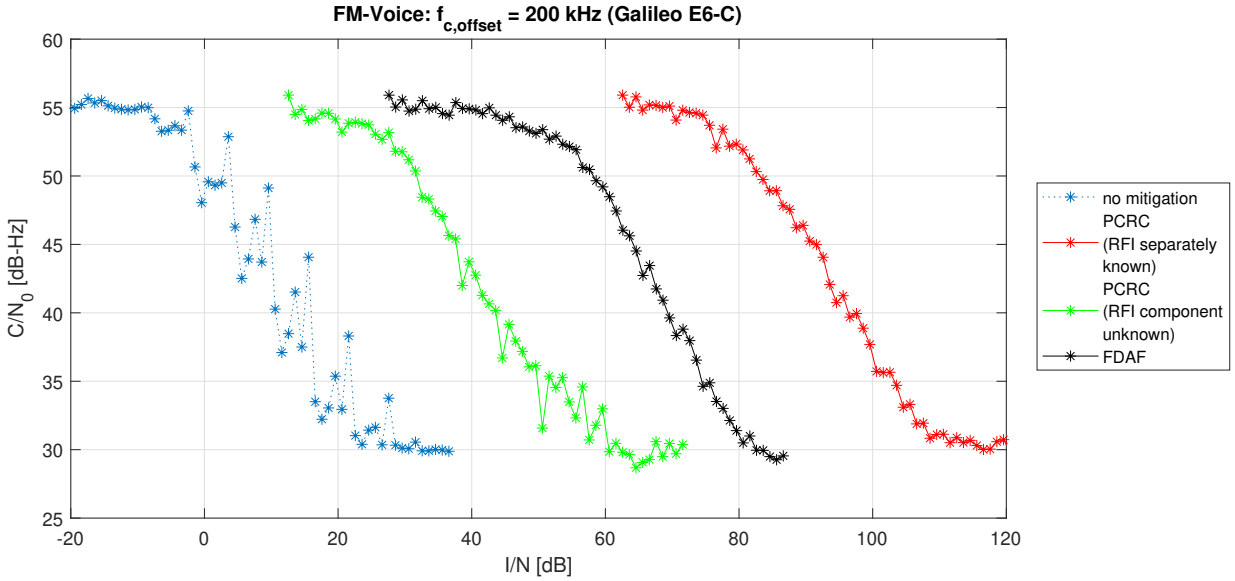

Figure 8: Performance comparison of interference mitigation with Galileo E6-C and a FM-Voice signal as interference

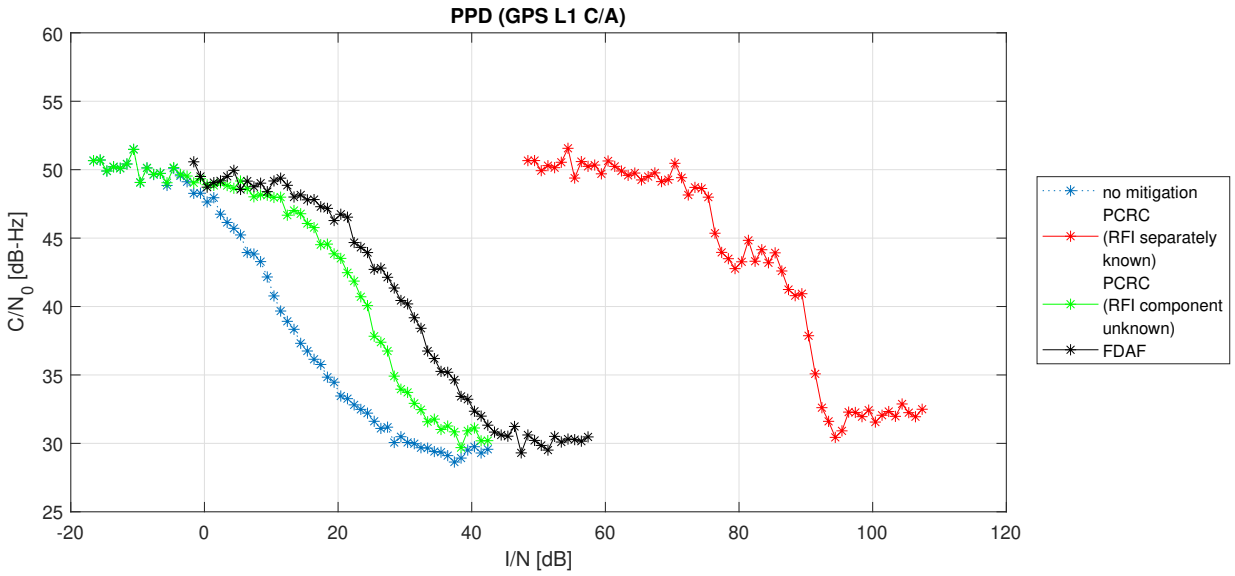

Figure 9: Performance comparison of interference mitigation with GPS L1-C/A and a PPD as interference

Figure 8 shows the effective C/N_0 for the Galileo E6-C signal, when FM-voice as interference is applied with and without of a mitigation technique. The central frequency of the FM-voice signal has an offset of 200 kHz to the transmitted center frequency of Galileo E6. Actually, the frequency offset in reality is at least 18 MHz as defined in the recommended IARU band plan for region 1 [33]. But, the effect of the interference would be to small and not so meaningful for this paper. The blue curve provides the effective C/N_0 without any protection. Normally, there is a steady-going degradation by the increase of the interference level as it is the case in Figure 9. The degradation varies by 12 dB. It is assumed that this is caused by the change of the frequency due to the frequency modulation with the voice as information, which hits different spectrum lines of the code replica with strongly different values. When the PCRC (green) is applied, we see an improvement in between of 20 to 32 dB. Compared with the pre-correlation FDAF method (black), the robustness increases by further 25 dB. The potential of the PCRC method becomes visible by the red curve, which brings further 25 dB and in total a robustness of at least 70 dB compared to no RFI mitigation. In this situation, the limitation is given by MATLAB® and its internal accuracy of calculation. The estimation is done by using

the RFI signal stream sp_{RFI} directly instead of the input stream sp_{in} for the I&D RFI estimator and it shows the maximum performance, which could be achieved by a perfect separation of the RFI from the GNSS noise floor. The processing in the frequency domain enables a higher degree of freedom, which might solve the separation with future research. The original idea was to distinguish the interference with the support of different spreading codes. During the work of this topic, it figured out that there is still the issue of separation. A second code just means a different amplitude and phase of the individual spectral line components. Another idea is to including more than one integration time intervals by superposition. Normally, every integration interval is only considered on its own. It is even possible to remove the GNSS energy by superposition, so that only the combined RFI information of both time intervals remains. By optimization of the GNSS signal design, there could also be a solution for an improved differentiator. Finally, the symmetry of the GNSS could be used. The positive and the negative frequency component of the GNSS modulation have the same amplitude, but because of the baseband processing both components are overlapping. Unfortunately, this also happens with the RFI components. To avoid this situation, the signal tracking must be done on an intermediate frequency. Such kind of IF correlator had been demonstrated once in [34].

Analog to the FM-voice example, Figure 9 shows the effective C/N_0 for the GPS L1-C/A signal, when a PPD as interference is applied with and without of a mitigation technique. This type of interference is more challenging for the GNSS signal tracking and interference mitigation, because it appears for a GNSS correlator as a broadband signal. The blue curve provides the effective C/N_0 without any protection. When the PCRC (green) is applied, we see an improvement of 12 dB. Compared with the pre-correlation FDAF method (black), the robustness increases by further 6 dB. The potential of the PCRC method becomes visible by the red curve, which brings further 42 dB and is similar to the absolute robustness of the narrow-band FM-voice signal.

VI. CONCLUSION

This paper introduced a novel concept to mitigate radio frequency interference (RFI) by the estimation of the RFI influence to the correlator. The estimation will be subtracted after the correlation process. This keeps the classical time domain tracking unit unchanged, which allows to activate the correction by estimation only in presence of the RFI to save additional computation effort. The estimation of the RFI occurs in the frequency domain. However, a inverse transformation is not needed. The feasibility was demonstrated by a software receiver and with real recorded signals. In this stage of work, this post-correlation RFI correction (PCRC) is only an academic approach and is not yet competitive with the classical pre-correlation FDAF method. But, there is a high potential to achieve higher performance of at least 70 dB protection against RFI. Some solution for future research had been discussed. The influence of spectral line components by RFI was visualized in a unique way, which provides a better understanding of how RFI is having an impact to the correlator result.

ACKNOWLEDGEMENTS

The results presented in this work were developed within the project *"Forschungs- und Studienvorhaben für Innovationen des Galileo GNSS-Systems (GalileoFusion)"* funded by the German Federal Ministry for Economic Affairs and Energy (BMWi) and administered by the Project Management Agency for Aeronautics Research of the German Space Agency (DLR) in Bonn, Germany (grant no. 50NA2001).

REFERENCES

[1] M. G. Amin, P. Closas, A. Broumandan, and J. L. Volakis, "Vulnerabilities, threats, and authentication in satellite-based navigation systems [scanning the issue]," *Proceedings of the IEEE*, vol. 104, no. 6, pp. 1169–1173, 2016.

[2] G. X. G. Sam Pullen, "GNSS Jamming in the Name of Privacy: Potential Threat to GPS Aviation," *insideGNSS*, no. 2, 2012.

[3] O. Towlson, D. Payne, P. Eliardsson, and V. Manikundalam, "D6.2: Threat Database Analysis Report," in *STRIKE 3 Project*, GSA, Ed., 2019. [Online]. Available: http://gnss-strike3.eu/downloads/STRIKE3_D6.2_Threat_database_Analysis_Report_public_v1.0.pdf

[4] GSA, Ed., *STRIKE 3 Project: Standardization of GNSS Threat reporting and Receiver Testing through International Knowledge Exchange Experimentation and Exploitation*, 2019. [Online]. Available: http://gnss-strike3.eu/

[5] Y. Li, J. Cervantes, N. C. Shivaramaiah, D. M. Akos, and M. Wang, "Configurable GPS/GNSS Antenna Module Resistant to RFI Saturation," *IEEE TRANSACTIONS ON AEROSPACE AND ELECTRONIC SYSTEMS*, vol. 56, no. 1, pp. 381–392, 2020.

[6] T. Kraus, T. Pany, and B. Eissfeller, "Maximum Theoretical Interference Mitigation Capability of a GNSS Receiver as Limited by the GNSS Frontend," *Proceedings of the 30th International Technical Meeting of The Satellite Division of the Institute of Navigation (ION GNSS+ 2017), Portland, Oregon*, pp. 3471–3480, September 25 - 29, 2017.

[7] G. X. Gao, M. Sgammini, M. Lu, and N. Kubo, "Protecting GNSS Receivers From Jamming and Interference," *Proceedings of the IEEE*, vol. 104, no. 6, pp. 1327–1338, 2016.

[8] C. Ouzeau, C. Macabiau, B. Roturier, and M. Mabilleau, "Performance assessment of multi correlators interference detection and repair algorithms for Civil Aviation," *ENC-GNSS 2008, Conference Europeenne de la Navigation, Apr 2008, Toulouse, France*, 2008.

[9] C. Ouzeau, "Degraded Modes Resulting From the Multi Constellation Use of GNSS," PhD, l'Institut National Polytechnique de Toulouse, Toulouse (France), 2010.

[10] D. Borio and P. Closas, "Robust transform domain signal processing for GNSS," *Navigation*, vol. 104, no. 6, p. 1302, 2019.

[11] T. Kraus, R. Bauernfeind, and B. Eissfeller, "Survey of In-Car Jammers - Analysis and Modeling of the RF Signals and IF Samples (Suitable for Active Signal Cancelation)," *Proceedings of the 24th International Technical Meeting of The Satellite Division of the Institute of Navigation (ION GNSS 2011), Portland, OR, September 2011*, pp. 430–435.

[12] R. H. Mitch, R. C. Dougherty, M. L. Psiaki, S. P. Powell, B. W. O'Hanlon, J. A. Bhatti, and T. E. Humphreys, "Signal Characteristics of Civil GPS Jammers," *Proceedings of the 24th International Technical Meeting of The Satellite Division of the Institute of Navigation (ION GNSS 2011), Portland, OR, September 2011*, pp. 1907–1919.

[13] A. J. Van Dierendonck, "GPS Receivers," in *Global Positioning System*, ser. Progress in astronautics and aeronautics, B. W. Parkinson and J. J. Spilker, Eds. Washington, DC: American Institute of Aeronautics and Astronautics, 1996, pp. 329–407.

[14] T. Pany, D. Dötterböck, H. Gomez-Martinez, M. S. Hammed, F. Hörkner, T. Kraus, D. Maier, D. Sanchez-Morales, A. Schütz, P. Klima, and D. Ebert, "The Multi-Sensor Navigation Analysis Tool (MuSNAT) – Architecture, LiDAR, GPU/CPU GNSS Signal Processing," in *Proceedings of the 32nd International Technical Meeting of the Satellite Division of The Institute of Navigation (ION GNSS+ 2019)*, ser. ION GNSS+, The International Technical Meeting of the Satellite Division of The Institute of Navigation. Institute of Navigation, 2019, pp. 4087–4115.

[15] T. Pany, *Navigation signal processing for GNSS software receivers*, ser. GNSS technology and applications series. Boston MA: Artech House, 2010. [Online]. Available: http://site.ebrary.com/lib/academiccompletetitles/home.action

[16] J. W. Betz, "Effect of Partial-Band Interference on Receiver Estimation of C/N0: Theory," in *Proceedings of the 2001 National Technical Meeting of The Institute of Navigation, Long Beach, CA, January 2001*, pp. 817–828.

[17] C. Macabiau, O. Julien, and E. Chatre, "Use of multicorrelator techniques for interference detection," *ION NTM 2001, National Technical Meeting, Jan 2001, Long Beach, United States*, pp. 353–363, 2001.

[18] F. Bastide, E. Chatre, and C. Macabiau, "GPS interference detection and identification using multicorrelator receivers," *ION GPS 2001, 14th International Technical Meeting of the Satellite*, pp. 872–881, 2001.

[19] C. Ouzeau, C. Macabiau, B. Roturier, and M. Mabilleau, "Performance of multicorrelators GNSS interference detection algorithms for Civil Aviation," *ION NTM 2008, 28-30 January 2008, San Diego, CA*, pp. 142–153, 2008.

[20] J. Jang, M. Paonni, and B. Eissfeller, "CW Interference Effects on Tracking Performance of GNSS Receivers," *IEEE TRANSACTIONS ON AEROSPACE AND ELECTRONIC SYSTEMS*, no. VOL. 48, NO. 1, pp. 243–258, 2012.

[21] M. Bek, S. Elgamel, E. Shaheen, and K. El-Barbary, "Interference Effect on the Post-Correlation Carrier to Noise Ratio for GPS Receiver," *The International Conference on Electrical Engineering*, vol. 9, no. 9th, pp. 1–15, 2014.

[22] M. K. Bek, E. M. Shaheen, and S. A. Elgamel, "Mathematical analyses of pulse interference signal on post-correlation carrier-to-noise ratio for the global positioning system receivers," *IET Radar, Sonar & Navigation*, vol. 9, no. 3, pp. 266–275, 2015.

[23] E. M. Shaheen and S. A. Elgamel, "Mathematical analyses of the GPS receiver interference tolerance and mean time to loss lock," *Defence Technology*, vol. 15, no. 3, pp. 440–449, 2019.

[24] K. Borre, *A software-defined GPS and Galileo receiver: A single-frequency approach*, ser. Applied and numerical harmonic analysis. Boston: Birkhauser, 2007.

[25] GNSS Laboratory, "SDR Code Update to Enable I/Q Complex Date Processing," 2008. [Online]. Available: https://ccar.colorado.edu/gnss/files/SDRcodeUpdate.pdf

[26] P. W. Ward, "GNSS Receivers," in *Understanding GPS/GNSS*, ser. GNSS technology and applications series, E. D. Kaplan and C. J. Hegarty, Eds. Boston and London: Artech House, 2017, pp. 339–548.

[27] GSA, *Galileo E6-B/C Codes: Technical Note*, issue 1 ed., 2019.

[28] T. Kraus, S. Sailer, and B. Eissfeller, "Modul zur Unterdrückung von Störsignalen für globale Navigationssysteme mit NI SDRs," in *Virtuelle Instrumente in der Praxis 2015*, R. Jamal and R. Heinze, Eds. Berlin and Offenbach: VDE-Verl., 2015, pp. 43–46.

[29] P. T. Capozza, B. J. Holland, T. M. Hopkinson, and R. L. Landrau, "A Single-Chip Narrow-Band Frequency-Domain Excisor for a Global Positioning System (GPS) Receiver," *IEEE JOURNAL OF SOLID-STATE CIRCUITS*, no. VOL. 35, NO. 3, 2000.

[30] BNetzA, "Coexistence measurements: amateur radio service and Galileo E6 in the frequency range 1260 – 1300 MHz: Measurement report G 001/00261/18 and G 531/00282/18 BNetzA, Germany," no. FM44(19)017, 2019. [Online]. Available: https://cept.org/Documents/fm-44/51132/fm44-19-017_proposals-for-coexistance-of-rnss-and-amateur-service-1240-1300mhz

[31] "Summary of SE40#65: Compatibility between RNSS and amateur service (1240-1300 MHz)," 2019-09-12. [Online]. Available: https://cept.org/ecc/groups/ecc/wg-se/se-40/news/summary-of-se4065/

[32] J. W. Betz, "Effect of Narrowband Interference on GPS Code Tracking Accuracy," *Proceedings of the 2000 National Technical Meeting of The Institute of Navigation*, pp. 16–27, January 26 - 28, 2000.

[33] ON4AVJ, "IARU Region 1 UHF band plan," 2020. [Online]. Available: https://www.iaru-r1.org/wp-content/uploads/2020/03/UHF-Bandplan.pdf

[34] C. YANG, "Sharpen the Correlation Peak: A Novel GNSS Receiver Architecture with Variable IF Correlation," *Navigation*, vol. 63, no. 3, pp. 249–265, 2016.